Hindawi
Advances in Multimedia
Volume 2023, Article ID 9892737, 1 page
https://doi.org/10.1155/2023/9892737

Retraction

Retracted: The Application of 3D Virtual Technology in the Teaching of Clinical Medicine

Advances in Multimedia

Received 12 December 2023; Accepted 12 December 2023; Published 13 December 2023

This article has been retracted by Hindawi, as publisher, following an investigation undertaken by the publisher [1]. This investigation has uncovered evidence of systematic manipulation of the publication and peer-review process. We cannot, therefore, vouch for the reliability or integrity of this article.

Please note that this notice is intended solely to alert readers that the peer-review process of this article has been compromised.

Wiley and Hindawi regret that the usual quality checks did not identify these issues before publication and have since put additional measures in place to safeguard research integrity.

We wish to credit our Research Integrity and Research Publishing teams and anonymous and named external researchers and research integrity experts for contributing to this investigation.

The corresponding author, as the representative of all authors, has been given the opportunity to register their agreement or disagreement to this retraction. We have kept a record of any response received.

References

[1] H. Zhang, J. Kong, Y. Tong, C. Gao, and W. Huang, "The Application of 3D Virtual Technology in the Teaching of Clinical Medicine," *Advances in Multimedia*, vol. 2022, Article ID 7979128, 11 pages, 2022.

Hindawi
Advances in Multimedia
Volume 2022, Article ID 7979128, 11 pages
https://doi.org/10.1155/2022/7979128

Research Article

The Application of 3D Virtual Technology in the Teaching of Clinical Medicine

Haifeng Zhang,[1] Juan Kong,[2] Yan Tong,[2] Chunmei Gao,[2] and Wei Huang[1]

[1]*Mudanjiang Medical University, Mudanjiang 157011, China*
[2]*The Second Affiliated Hospital of Mudanjiang Medical University, Mudanjiang 157000, China*

Correspondence should be addressed to Juan Kong; 160701221@stu.cuz.edu.cn

Received 18 August 2022; Revised 5 September 2022; Accepted 14 September 2022; Published 29 September 2022

Academic Editor: Tao Zhou

The booming development of 3D virtual technology provides the basis for the innovation of teaching mode of clinical medicine. Integrating 3D virtual technology into the clinical education teaching of medical students can help medical students learn clinical expertise more intuitively, enrich practical experience, improve hands-on ability, and make up for the shortcomings of traditional medical teaching. However, the traditional 3D modeling method has the problems of sparse and insufficient accuracy of output results, which greatly limits the specific application of 3D virtual technology in clinical teaching. Therefore, this paper addresses the shortcomings of previous 3D virtual technology in 3D modeling of organs, introduces deep learning, and then proposes a pyramidal shape perception network with the ability to generate samples on point clouds. Experimental results show that the proposed model not only has a large improvement in accuracy but also shows a high degree of confidence in providing real-time feedback of local image attributes.

1. Introduction

In traditional clinical teaching, the teaching effect of clinical medicine is affected by how many hands-on opportunities medical students have. The problems of unrealistic anatomical models and the lack of solid specimens are still evident. Medical students rely more often on anatomical atlases, CT images, and teaching videos to teach and learn, making it difficult to transfer knowledge and learn to master in-depth [1]. In addition, the opportunity and time for students to do hands-on work are significantly reduced due to the prominence of acute doctor-patient conflict, and the reality of clinical medicine teaching faces more realistic problems. Traditional clinical medicine teaching faces more significant challenges. With the development of economic and social progress, the demand of patients for medical resources is also increasing, conventional teaching methods can no longer meet the needs of clinical teaching, and innovative teaching methods and exploration of new teaching modes have become an essential topic for clinical medical education.

As the use of 3D virtual technology becomes more widespread, clinical medicine is beginning to incorporate the technology into its educational innovations [2]. The 3D imaging technology and naked-eye 3D to present the structure of human tissues, organs, and systems have improved the teaching level of clinical medical education and endowed clinical medical education with new teaching methods and technical means. Especially in clinical medicine, competent medical care's intuitive and clear technical advantages have greatly improved students' motivation and learning effect. For example, 3D printing technology has alleviated the current situation that human anatomy learning is limited by various biological specimens and the insufficient number of human specimens. Virtual reality technology allows medical students to immerse themselves in the learning process of surgery, which makes the learning efficiency greatly improved and, at the same time, gives medical students effective consolidation and review opportunities. In other words, 3D virtual technology has excellent potential for application in teaching clinical medicine [3]. However, there

are still many problems in applying 3D virtual technology in clinical medicine, which significantly limits its specific application in clinical medicine teaching. For example, the accuracy of 3D visualization is not sufficient and needs to be assisted with additional information such as anatomical images. Another example is that the complex steps of 3D modeling of surgical organs, including preprocessing, alignment, and coordinatization, reduce the automation of hardware and software, limiting the application of visualization devices for teaching scenarios.

Therefore, this paper attempts to combine deep learning methods' powerful feature extraction and nonlinear fitting capabilities to autonomously learn the high-dimensional nonlinear mapping relationship between traditional medical image input and brain 3D point cloud output and to achieve the synthesis of high-quality, low-error 3D point clouds from as few 2D images as possible in order to solve the problem of insufficient clinical visual information in practical applications and provide a technical basis for teaching clinical medicine.

2. Literature Review

This paper firstly reviews the research progress of 3D virtual technology in the medical field, secondly composes the advancement of 3D virtual technology in clinical medicine teaching, and finally emphasizes the value and significance of 3D virtual technology for clinical medicine teaching.

2.1. 3D Virtual Technology and Medicine. Currently, the 3D virtual technologies widely used in the medical field mainly include 3D printing technology and virtual reality (VR) and augmented reality (AR) technologies.

2.1.1. 3D Printing Technology. 3D printing is a new additive manufacturing technology, and medical 3D printing refers to using volumetric datasets to model anatomical structures for medical applications [4]. 3D printing technology can produce highly complex, patient-specific models of structures that are difficult to produce using traditional manufacturing techniques, including injection compression molding, solvent casting, porogenic dissolution, and electrostatic spinning, which are challenging to achieve. 3D printing technology is currently used in several medical fields, including dental and surgical specialty anatomical models, medical instruments and tools, tissue engineering scaffolds, and drug production. Within these fields, dental and hearing aid industry applications are the most popular, probably due to the small size of the finished products and the need for unique design, which 3D printing technology can meet. Surgical applications include medical devices, surgical instruments, and anatomical models. 3D printing technology is also being applied to pharmaceuticals as the industry places increasing emphasis on the development of personalized medicines. At the same time, 3D printing is becoming increasingly popular in tissue engineering and regenerative medicine. In addition, biological 3D printing of tissue models and disease models for drug testing is proliferating, not only to develop more personalized drugs for patients but also to reduce the use of animal models in animal testing.

The general steps of medical 3D printing include acquiring medical imaging data, modeling, and outputting to a printer for printing and postprocessing. The acquisition of medical imaging data, including computed tomography (CT), magnetic resonance imaging (MRI), or 3D ultrasound, are traditional means of examination [5]. The accuracy and quality of the acquired medical imaging data are increasing with the improvement and upgrading of equipment, which facilitates the next step of modeling with higher accuracy. In the past, due to confidentiality and technical reasons, these images could only be viewed within the hospital. Still, with the development of data storage technology and the corresponding cost reduction, many hospitals have started to provide source data copy services, making it more and more convenient to obtain data, which is conducive to the flow of medical image data and thus to data reprocessing and utilization. Modeling, short for building digital models, refers to the application of modeling software to generate three-dimensional digital models of medical imaging data in two dimensions. The modeling software often used in clinical medicine includes Mimics (materializes the interactive medical image control system, Materialise, Belgium) and 3D Slicer (open source software). Some domestic companies have also developed their artificial modeling software (e.g., United Imaging, Inc.). Modeling mainly consists of two steps: image segmentation and 3D model generation; firstly, image segmentation, i.e., extraction of the region of interest from the 2D source image, and then superimposition into a 3D digital model and conversion into STL (Standard Tessellation language or Stereo Lithography) file format. The STL file format is the first and most commonly used 3D file format supported by 3D printers, in addition to the AMF (additive manufacturing file) format published by the American Society for Testing and Materials (ASTM) and the AMF (additive manufacturing file) format published by Microsoft in conjunction with HP and 3D Systems. In addition, there is the AMF (additive manufacturing file) format issued by the American Society for Testing and Materials (ASTM) and the 3MF format launched by the 3MF Consortium, a consortium of Microsoft, HP, 3D Systems, Stratasys, Materialise, and other giants.

2.1.2. VR and AR Technologies. With the successful development of computer graphics, spatial positioning tracking, and other technologies, VR technology, which was born on this basis, started to be applied to the medical field [6]. VR technology refers to the use of a specific display device that presents the user with a particular display device that offers the user an utterly virtual scene with pregenerated stereoscopic images that the user can interact with through various sensors. This allows clinicians to use VR technology to presimulate the surgical site, thereby effectively reducing the risk of surgery due to subjective predictions by the surgeon, unclear preoperative patient communication, and unskilled intraoperative operations. Further effective preoperative processing of the original medical images of patients (e.g., medical 3D reconstruction, surgical path planning, and preoperative simulation rehearsal) has gradually become the trend in clinical medical surgery [7].

AR is a brand-new technology further developed based on VR, which extends the human visual perception of the natural environment by accurately superimposing computer-generated virtual objects or other auxiliary information into the actual scene and allowing users to interact with this virtual information fused to the real world in real time, thus completing the "augmentation." Meanwhile, thanks to the rapid improvement in the performance of smartphones, tablets, and other wearable mobile devices, as well as the increasing maturity of computer vision and mobile cloud computing and other technologies on mobile devices, combined with various advanced sensors and ubiquitous and stable network connections, AR technology continues to move toward the more convenient mobile augmented reality (MAR). Compared with virtual reality, mobile augmented reality appears to be more practical in the medical field. The virtual reality scenario is entirely computer-generated, and the operation scenario during the virtual surgery does not match the reality. However, mobile augmented truth does not exclude the doctor's original real-world view but only opens up a new perspective (i.e., the overlay of the virtual medical 3D model and the initial real world), and the virtual model and the natural world not only match each other but also can achieve instant interaction. The two types of information correct each other, making the surgery much safer and more accurate. Although the application of mobile augmented reality technology in the medical field is still in the preliminary exploration stage, the current mobile augmented reality technology also has many shortcomings: such as network latency, data management, system stability, device endurance [8], virtual-real alignment accuracy, security privacy, and social acceptance and other issues need to be further improved. However, the digital, individualized, minimally invasive, and remote characteristics of mobile augmented reality technology are very much in line with the current direction of medical development and show excellent application prospects. We believe that the emergence of mobile augmented reality technology will bring significant changes in traditional medical education, doctor-patient communication, remote consultation, and surgical safety and greatly promote the arrival of the medical innovation and change era [9].

In AR systems, real and virtual objects are combined to form a comprehensive visualization system. Virtual objects correspond to patient-specific models, plans, and preoperative images. The actual objects correspond to the surgical field of view, which can be captured by an external camera, surgical microscope, or endoscope. The real world is then merged with the virtual objects to create the visualization of AR. The use of AR in clinical medicine serves two purposes: first, AR provides a visualization that maps preoperative images of the neurological display onto the patient, and through AR technology, clinicians can see the relevant anatomical structures beneath the patient's visible surface. In addition, reliance on autopsy and theoretical training will inevitably lead to slow surgical progress. The disadvantage of traditional neurosurgery is that the clinician must divert attention from the patient to the monitor for guidance, leading to distraction's undesirable effect [10]. Therefore combining real-world surgical scenarios with preoperative virtual patient images and planning is an effective way to address this drawback. AR technology is currently used for simulation and training in clinical medicine surgery. Although the application of AR in clinical practice is still in its infancy, it is gradually becoming widely accepted and used.

2.2. 3D Virtual Technology in the Teaching of Clinical Medicine. 3D printing technology is widely used in the teaching of clinical medicine. Traditionally, teachers have had to use human cadavers in order to accurately and visually teach students anatomy and the morphological relationships of various organs in medicine. However, it is difficult to gain sufficient surgical experience to treat a variety of diseases using this method. Assisting and observing surgical procedures provides young physicians with indirect experience, but this approach is not sufficient to improve operative skills and visual understanding of complex pathologies and diseases (especially anatomical details), a deficiency that is more pronounced in surgical learning using laparoscopy and endoscopy. Therefore, many young surgeons must develop their surgical skills during real surgical procedures. On the other hand, however, it is increasingly difficult to dissect human cadavers or observe medical treatments due to cultural objections to dissection and the strengthening of patients' rights, which is even more detrimental to medical students' learning. As a result, personalized 3D printed models of patients are increasingly being used to train young surgeons in surgical procedures, including orthopedic surgery, endovascular stenting, live bile duct drainage, and neurosurgery. Advances in multimaterial 3D printing technology allow for increasingly realistic models that simulate real hard and soft tissues. It has been found that the use of neurosurgical multimaterial printed models with different properties and densities can be used by trainees to practice not only the basic surgical steps but also the full range of steps from navigation and skin flap planning to craniotomy and simple tumor removal [11, 12]. Thus, the application of 3D printing has the potential to have a significant impact in the field of neurosurgery. Two major problems with neurosurgical training in the past have been that shorter working hours, increased numbers of physicians in training, and legal issues have reduced opportunities for trainees to practice under direct supervision and that current endoscopic neurosurgery training often uses cadavers and simulation models that lack pathology or realism, making it impossible to ensure the effectiveness of training. Using 3D printing technology, pathology models can be created using imaging data from actual patients and reproduced in large numbers. These models provide a safe, realistic environment for teaching neuroendoscopic surgery and can directly address both of these issues.

The application of VR and AR technologies in clinical medicine teaching has also been rapidly developed. VR technology is particularly suitable for medical and educational applications because of its own characteristics, creating a virtual learning space through science and technology, transforming abstract knowledge into real experience through virtual sensory and virtual visualization, and establishing an innovative teaching model. In addition to more accurate, comfortable, and ergonomic VR equipment, the reproduction of

real clinics also requires multisensory feedback devices; e.g., for virtual clinical patient examination training, in addition to visual input, accurate tactile and auditory feedback on the patient's body texture and internal organ auscultation sounds are also required. The advantages of VR and AR technologies in clinical education include the following [4]: (1) realistic simulation of clinical situations and feedback; (2) large number of medical students can be exposed to the teaching content at the same time; (3) clinical teaching will no longer be limited by time and space, and the autonomy is more reasonable; and (4) VR/AR teaching content can be reused once recorded and can reduce the cost of training operations in real space. Based on the characteristics and development trend of VR and AR technologies, and the way VR and AR technologies are linked with medical education, VR and AR technologies are suitable for teaching clinical medicine courses. Current research shows that the application of VR technology in the field of medical education has good results and high acceptance [13].

In conclusion, researchers have increasingly focused on 3D printing technology and VR/AR technology in recent years. Their broader application in clinical medicine education allows medical students to practice in a controlled environment, thus avoiding severe errors. 3D printing technology and VR/AR technology can play a great role in organ reconstruction, surgical scene simulation, etc., thus helping to realize three-dimensional clinical medical teaching. However, with the increasing precision requirements of clinical surgery, the traditional 3D reconstruction technology can no longer meet the practical needs of teaching, and the construction of higher-order 3D reconstruction technology is necessary.

3. Methodology

3D reconstruction of organs is essential in clinical medicine teaching. As the current medical requirements for surgical precision increase, the output of traditional 3D reconstruction methods (e.g., point cloud reconstruction) faces the problems of too sparse and insufficient precision. In addition, there are too few high-density point cloud datasets that meet the density requirements of these surgeries, and it is difficult to directly train models to reconstruct high-density point clouds. Therefore, we propose a novel model called pyramid shape perception network based on an improved generative adversarial network, which consists of a feature extraction encoder and two GANs with a two-stage generation process for generating accurate high-density point clouds with a single image as the input condition. The first stage GAN outlines the original shape and basic structure of the organ based on the given image to produce the first stage low-density point cloud. The second stage GAN takes the results of the first stage and produces a high-density point cloud with details. The second stage GAN is able to correct the defects and recover the details of the target organ through the point cloud upsampling process. In addition, a parameter-free transforming module (FTM) based on computational spatial attention is proposed in this chapter to extract high-quality image input features while ensuring the performance of the model.

3.1. WGAN. Generative adversarial network (GAN) has been facing the following problems and challenges since its introduction [14]: (1) training is difficult, requiring careful design of the model structure and careful coordination of the training level of the generator and discriminator; (2) the loss functions of the generator and discriminator do not indicate the training process and lack a meaningful metric to correlate with the quality of the generated images; and (3) mode collapse, where the generated images lack diversity although they look real, but lack diversity. Under such a premise, the Wechsler generative adversarial network (WGAN) was created. Normally, the conventional loss function of GAN is as follows [15]:

$$L_G = E_{z\sim Z}[\log(1 - D(G(z)))], \tag{1}$$

$$L_D = E_{z\sim Z}[\log(1 - D(G(z)))] + E_{Y\sim R}[\log(D(Y))]. \tag{2}$$

The optimization of the above objective function is equivalent to minimizing the Jensen-Shannon (JS) scatter between the real and synthetic data distributions [16]. WGAN introduces the Wasserstein distance/Earth mover's distance into the training by improving the loss function as

$$L_G = -E_{z\sim Z}[D(G(z))], \tag{3}$$

$$L_G = E_{z\sim Z}[D(G(z))] - E_{Y\sim R}[D(Y)]. \tag{4}$$

This is to approximate the Wechsler distance between the two networks so that the distance between the input and output distributions can be measured in probability space, which can guide the network training more rationally.

The main reason is the Lipschitz continuity condition, and WGAN is an improvement for the Lipschitz continuity condition. WGAN has only two changes compared to GAN: (1) WGAN cuts the weights of the training parameters, while WGAN uses the gradient penalty to update the parameters. WGAN uses gradient penalty to update the parameters, so that the weights can be evenly distributed and the learning power of the neural network can be fully exploited; (2) the discriminator does not use batch norm, because each sample is independently added with gradient penalty, while batch norm introduces dependency between samples of the same batch. With this enhancement, the WGAN network really improves the problem of pattern collapse in traditional GAN networks [17, 18].

3.2. PSP-GAN. We propose a pyramid-shape-perception generative adversarial network (PSP-GAN) for the task of high-density point cloud reconstruction in a limited surgical visual environment. This is the first work to introduce a point cloud upsampling algorithm in 3D brain reconstruction to improve the accuracy of the reconstruction. We also propose a model that can ensure the precise perception of the 3D shape. In addition, we designed a correct reconstruction framework that works in a pyramidal layer-by-layer generation. The model extracts image features and builds a

first-stage generator based on a tree-structured GCN module that describes the branching structure of point features and outlines the basic shape of the object. The model also builds a second-stage generator based on dense GCN modules, which contains an aggregation step, an upsampling step, and a coordinate reconstruction step to refine the object details in the first stage and correct errors. Based on this strategy, it can effectively and sensitively perceive the delicate shape and structure of the brain. Finally, unlike traditional attention mechanisms that require additional computational parameters, we designed a parameter-free transfer machine module that uses parameter-free self-attention to improve accuracy while ensuring efficient models [19]. It is adapted to surgical scenarios where model processing time is sensitive to take advantage of the data properties of point cloud representations and reduce reconstruction errors.

The overall structure of our proposed pyramid shape perception network is shown in Figure 1. The pyramid shape perception network consists of an encoder based on a parameterless transfer machine module and two generative adversarial network structures. In the first stage, GAN generates the first stage sparse point cloud by sketching the object's original shape and basic structure based on the given image. In the second stage, GAN uses the results of the first stage as input to generate a high-density point cloud with details. In the second stage, GAN only needs to correct the defects and recover the target details by upsampling the point cloud, thus avoiding the reconstruction error of direct generation. Considering each module's input and output differences, we design a unified information flow to communicate with neighboring modules.

In general, a generic generative adversarial network framework aims to learn a generative model where an encoder can be extended to the model to aggregate the corresponding input features to generate a low-dimensional generative factor [20]. And this representation factor can be considered a stream of information capturing the necessary details of the input. Therefore, we use an attentional network and introduce a parameter-free attentional mechanism to enhance its feature extraction capability and maintain its computational performance. The constructed network is called a parameter-free transformer module (FTM). Compared with the traditional attention block or transformer structure, FTM considers how to reduce the consumption of computational resources by avoiding the introduction of additional computational parameters when computing the weight fraction representing the importance of features. Instead, the FTM attempts to build a purely numerical computational attention network whose biological interpretation partially corresponds to the way human brain neurons work (Figure 2).

Different signal firing patterns or suppression of firing from a neuron's peripheral neurons are often possible markers of high activity in that neuron [21]. Following similar guidelines, we constructed a similar attention mechanism to guide the deep neural network to adjust the weights according to a linear separability computation between one target and other targets. Given a particular feature T_k located at the kth layer in the network, we define the energy function e_t of any element t in the feature matrix T as

$$e_t = \frac{1}{\#c^k - 1} \sum_{i=1}^{\#c^k - 1} \left(-1 - \left(w_t t_i + b_t\right)\right)^2 + \left(1 - \left(w_t t + b_t\right)\right)^2 + \lambda w_t^2, \tag{5}$$

where $\#C^k$ is the number of elements in the channel where t is located, which can also be calculated as $H_k * W_k$. $w_t t_i + b_t$ and $w_t t + b_t$ are linear transformations of t_i and t. $\lambda {w_t}^2$ is a canonical term. We can find the linear separability between the target and all other elements in the same channel by minimizing this energy function.

We calculate for each channel only a mean μ_C and a variance ${\sigma_C}^2$ and use this result when calculating all elements of the same channel. They can be described as

$$\mu_C = \frac{1}{\#c^k} \sum_{i=1}^{\#c^k} t_i, \tag{6}$$

$$\sigma_C^2 = \frac{1}{\#c^k} \sum_{i=1}^{\#c^k} \left(t_i - \mu_C\right)^2. \tag{7}$$

Therefore, the attention fraction a_t of element t can be calculated as

$$a_t = \frac{4\left(\sigma_C^2 + \lambda\right)}{\left(t - \mu_C\right)^2 + 2\left(\sigma_C^2 + \lambda\right)}. \tag{8}$$

The more general implication of attention scores is that the higher the score, the more important the element, which is inconsistent with the minimization goal of the current definition of attention scores [22]. Therefore, we unify the model of the attention mechanism by defining the reciprocal of the current attention score as the new attention score, which can be described as

$$a_t = \frac{\left(t - \mu_C\right)^2 + 2\left(\sigma_C^2 + \lambda\right)}{4\left(\sigma_C^2 + \lambda\right)}. \tag{9}$$

By calculating the attention score for each element, we are able to gradually obtain an attention score map A_k, which is similar to the traditional attention mechanism, but our attention score map is defined for each element, not just channel-wise or spatially, which also makes it more sensitive to subtle microstructural changes in medical images. After obtaining the entire attention score map, we adjust the output weights of network layer k according to the following formula:

$$T^k \longleftarrow \operatorname{softmax}\left(A^k\right) \times T^k. \tag{10}$$

We add this attention mechanism after each intermediate layer of a primary ResNet network, tune the model elements one by one to make them more accurate, and use this network as a backbone to build an FTM to compose our encoder [23]. Our encoder can thus extract the features of the input image compassionately. In contrast to

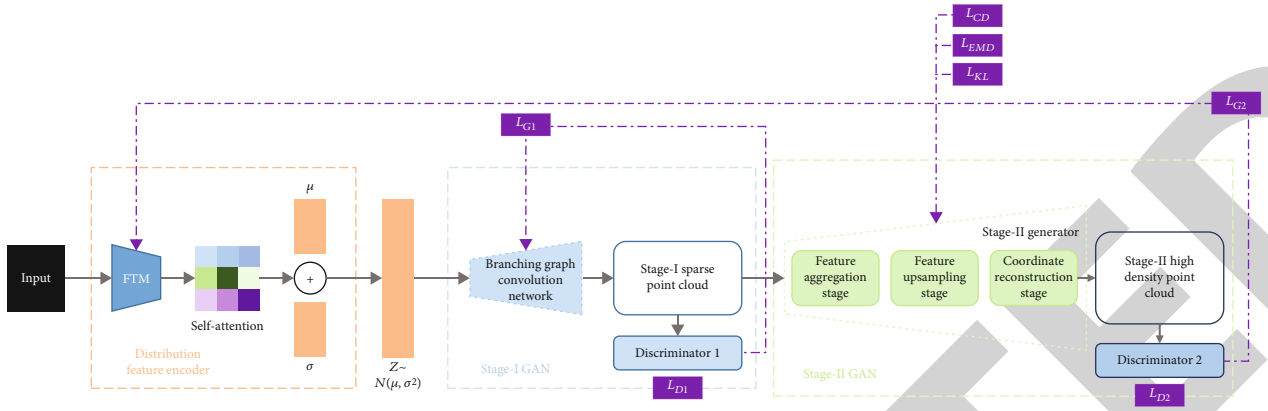

Figure 1: The architecture of the proposed model.

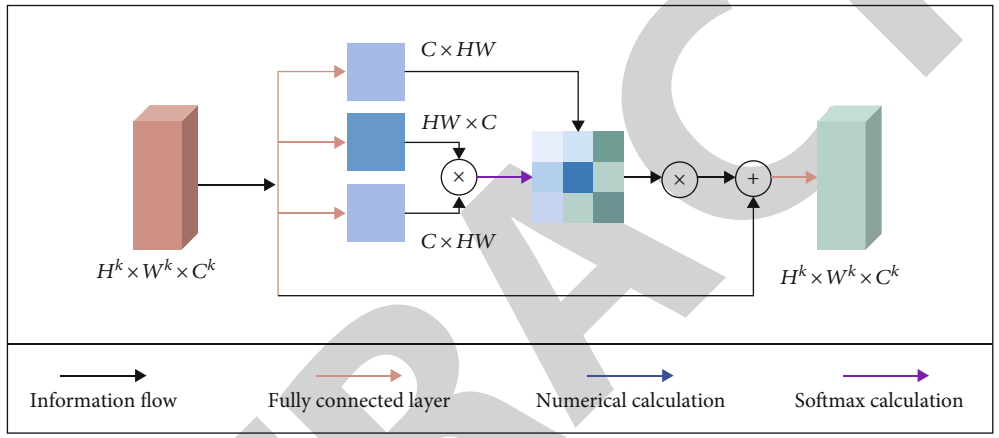

Figure 2: Traditional self-attention mechanism.

traditional attention networks, our FTM does not introduce additional parameters to support the acquisition of attention scores; all mappings are computed numerically. In this way, we ensure temporal sensitivity (Figure 3).

Given that MRI images contain a wealth of information, the first step in 3D reconstruction is to recover the physical structure represented by these images. The FTM-based encoder can extract a wealth of geometric information, which is then used by the subsequent network to reconstruct as close to the real point cloud as possible.

After the first stage of the GAN has understood the feature vectors and generated low-density point clouds, the second stage of the GAN is designed to accomplish upsampling of the point clouds to reconstruct high-density point clouds to support more complex brain-machine interface surgeries. Considering the advantages of GCN in point cloud tasks, we still use the basic GCN module as the skeleton to build this second-stage generator. Unlike the first-stage generator, the point cloud upsampling process is more of a "top-down" feature aggregation and feature generalization process, which a tree structure generator cannot fully exploit. Therefore, the second stage generator is designed as a stack structure with three processes: feature extraction, feature upsampling, and coordinate reconstruction. The low-density point cloud is expanded point by point in the form of an information flow and reconstructed into a high-density point cloud with a credible brain microstructure.

By designing components with basic GCN blocks, we built a stack-structured GCN to complete the upsampling process of point clouds [24]. In this process, we refine the brain's point cloud output details. At the same time, we corrected some possible errors in the stage one point cloud details by designing different loss functions. The structures of the first- and second-stage generators are shown in Figure 4.

To train the generators and discriminators in an adversarial manner, we use the WGAN strategy described above.

$$L_G = -E[D(G(f))], \tag{11}$$

$$L_D = E[D(G(f))] - E_{Y \sim R}[D(Y)] + \lambda_{gp} E_x \left[\left(\| \vee_x D(x) \|_2 - 1 \right)^2 \right]. \tag{12}$$

Generator 1 is trained directly using LG, and discriminator 1 and discriminator 2 are trained directly using LD, while encoder and generator 2 are trained obeying the loss function:

$$L_U = \lambda_1 L_G + \lambda_2 L_{KL} + \lambda_3 L_{CD} + \lambda_4 L_{\mathrm{EMD}}, \tag{13}$$

where λ_1, λ_2, and λ_3 are the weighting coefficients.

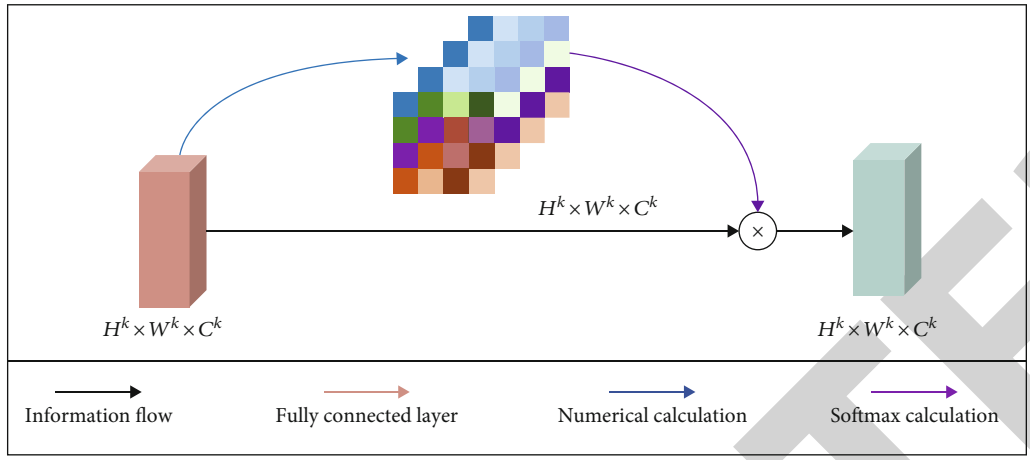

Figure 3: Parameter-free self-attention mechanism that constitutes our FTM.

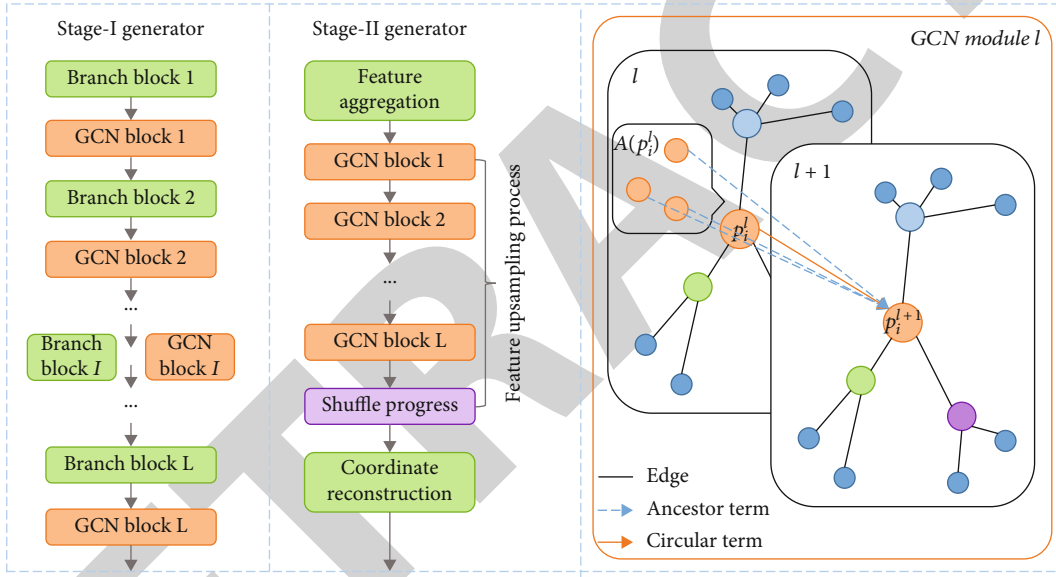

Figure 4: The structure of the stage I generator and stage II generator.

In sum, we propose a new type of image-point cloud upsampling reconstruction network called pyramidal shape perception network to address the low definition and density problems of existing 3D reconstruction methods in order to improve the generality and robustness of 3D shape reconstruction techniques in surgical scenarios.

4. Discussion and Results

The experimental dataset in this chapter is constructed on an in-house dataset. The dataset consists of 232 MRI images of Alzheimer's disease brains and 684 MRI images of healthy brains. Preprocessing of the dataset was done under the professional supervision of a physician. We randomly selected 600 MRIs to construct the training set; the rest were used for testing. To better evaluate the performance of the proposed model, we selected several currently available state-of-the-art point cloud upsampling models for generation experiments under the same conditions and scenarios. They are PU-net, PUGAN, and 3PU. The experimental results are reported in the following. The model was implemented using PyTorch, and all experiments were performed on an Intel Core i9-7960X CPU @ 2.80 GHz ×32, and an Nvidia GeForce RTX 2080 Ti GPU.

To demonstrate the effectiveness and accuracy of our encoder based on the parameter-free transfer machine module, we have made the following two modifications: (1) "ResNet" is a network variant that eliminates the attention calculation; such a variant eliminates the self-attention mechanism of the encoder network. (2) "NormalNet" is the normal variant, replacing the parameter-free self-attentive computation structure. The overall error comparison results are shown in Figure 5.

We further change and observe the effect of different first-stage generation systems on the model. Two modifications are also made as follows: (1) "No-D" is a variant that removes the discriminator of the first-stage generator, which eliminates the effect of adversarial generation. (2) "PointOutNet" is a variation

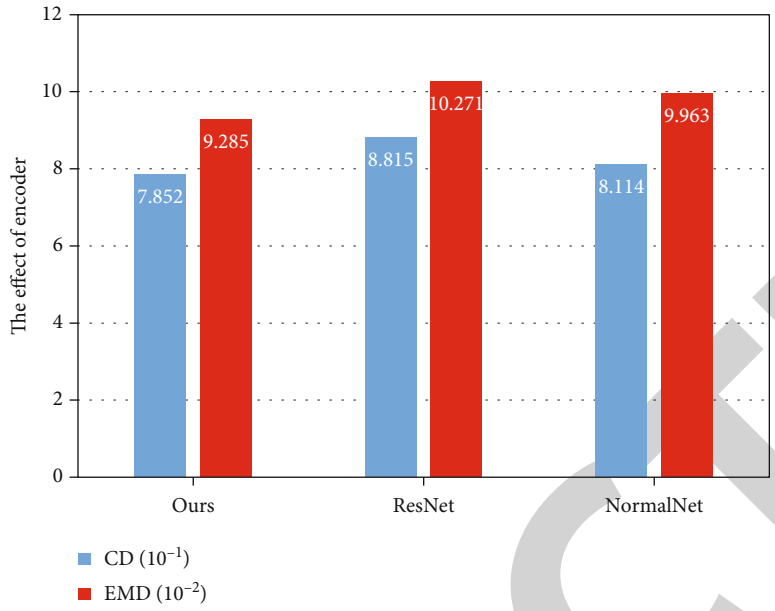

Figure 5: The effect of different encoder structure.

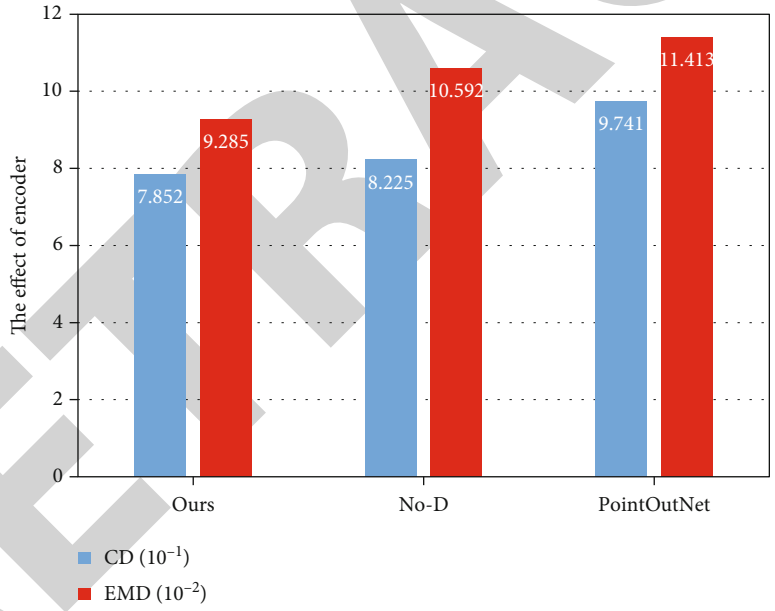

Figure 6: The effect of different stage I generating system.

of our first-stage adversarial network structure using PointOutNet, another point cloud generation architecture. The comparison results are shown in Figure 6, and it can be seen that the output of the proposed structure in this chapter has the slightest generation error. This proves that the proposed structure can best help the model achieve accurate 3D construction goals.

We also include FTM-based encoders in these experiments for comparison with other models: (1) "one-stage" refers to the variant that uses only the first-stage tree-graph convolution to generate the adversarial network directly the high-density point cloud. (2) "PU-Net" is a variant that uses PU-Net instead of the second-stage adversarial network. (3) "3PU" is a variation of the second-stage adversarial network generation using 3PU instead. (4) "PU-GAN" is a variant that uses PU-GAN instead of the second-stage adversarial network. We report the error results of the output of these variants in Figure 7, which also demonstrates the excellent performance of our proposed structure.

We conducted experiments using preprocessed 2D MRI and achieved good results. Considering that some existing models do not precisely match our experimental objectives, we added some modules to some other models in our comparison experiments to suit our experimental situation.

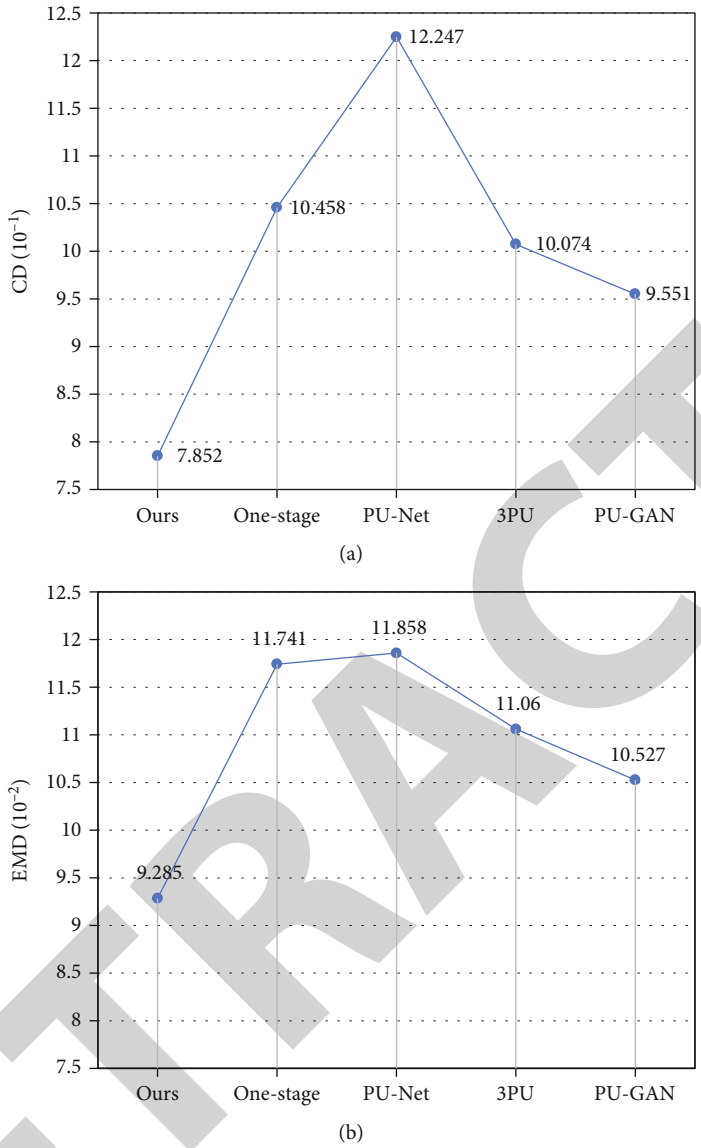

Figure 7: The effect of different stage II generating system.

The experimental structure proved the validity and credibility of our model. In our experiments, our model performs better than other state-of-the-art combinations. Our method has a short inference time and can effectively provide real-time feedback on local image properties. This feedback can improve the teachability of clinical medicine.

5. Conclusion

The 3D virtual technology has significantly remedied traditional clinical teaching problems, allowing students to apply the theoretical knowledge they have learned promptly in situational practice instead of just limiting themselves to books, effectively solving the issue of the disconnection between theory and practice in clinical medicine teaching. However, existing conventional medical images, such as CT and MRI, often suffer from at least one of two problems in clinical teaching: first, they are often incomplete due to light limitations and various possible visual contaminants outside the surgical plan (e.g., local bleeding). Second, their resolution does not always meet the exponentially increasing level of detail required for clinical teaching. Therefore, intraoperative organ 3D reconstruction techniques have been gradually developed.

To solve the problem that the output of traditional 3D reconstruction methods is too sparse and not accurate enough and the high-density point cloud dataset is too small, a pyramidal shape perception network with point cloud upsampling generation capability is proposed. The model has two stages for generating accurate high-density point clouds with a single image as input. The first stage of the generative adversarial network sketches the original shape and basic structure of the target organ based on the given image to generate the low-density point cloud in the first stage. The second stage of the generative adversarial network takes the results of the first stage and produces a high-

density point cloud with details. The second stage network is able to correct the defects and recover the details of the target organ through the point cloud upsampling process. In sum, the proposed model uses preprocessed 2D MRI to conduct various experiments addressing clinical teaching problems that can help medical students better grasp 3D shape and location information of organs and enrich their practical experience.

There are several limitations to the present research. First, the dataset we used is small, and future research can further expand the dataset to validate the robustness of the proposed model. Second, the proposed model still has many constraints that limit the model's ability to be applied across scenarios, so we hope that future research can help reduce the model's input constraints to eliminate the model's unavailability in more scenarios.

Data Availability

The labeled dataset used to support the findings of this study is available from the corresponding author upon request.

Conflicts of Interest

The authors declare that there are no conflicts of interest.

Acknowledgments

This work was sponsored in part by the following fund project: Effect of Blood Viscosity Coefficient on Hemodynamic Parameters of Cerebral Aneurysms Based on Numerical Simulation Method (2020-KYYWF-0814).

References

[1] P. Shah and B. S. Chong, "3D imaging, 3D printing and 3D virtual planning in endodontics," *Clinical Oral Investigations*, vol. 22, no. 2, pp. 641–654, 2018.

[2] L. Li, F. Yu, D. Shi et al., "Application of virtual reality technology in clinical medicine," *American Journal of Translational Research*, vol. 9, no. 9, pp. 3867–3880, 2017.

[3] S. Celi, E. Gasparotti, K. Capellini et al., "3D Printing in Modern Cardiology," *Current Pharmaceutical Design*, vol. 27, no. 16, pp. 1918–1930, 2021.

[4] X. Shao, Q. Yuan, D. Qian et al., "Virtual reality technology for teaching neurosurgery of skull base tumor," *BMC Medical Education*, vol. 20, no. 1, pp. 1–7, 2020.

[5] A. Zoabi, I. Redenski, D. Oren et al., "3D printing and virtual surgical planning in oral and maxillofacial surgery," *Clinical Medicine*, vol. 11, no. 9, p. 2385, 2022.

[6] A. Perin, T. F. Galbiati, R. Ayadi et al., "Informed consent through 3D virtual reality: a randomized clinical trial," *Acta Neurochirurgica*, vol. 163, no. 2, pp. 301–308, 2021.

[7] D. Popescu, R. Marinescu, D. Laptoiu, G. C. Deac, and C. E. Cotet, "DICOM 3D viewers, virtual reality or 3D printing–a pilot usability study for assessing the preference of orthopedic surgeons," *Proceedings of the Institution of Mechanical Engineers, Part H: Journal of Engineering in Medicine*, vol. 235, no. 9, pp. 1014–1024, 2021.

[8] J. Kim, Y. C. Lin, M. Danielak et al., "Virtual planning and rapid 3D prototyping surgical guide for anterior crown lengthening surgery: a clinical case report," *Journal of Prosthodontics*, vol. 31, no. 4, pp. 275–281, 2022.

[9] R. Tang, L. F. Ma, Z. X. Rong et al., "Augmented reality technology for preoperative planning and intraoperative navigation during hepatobiliary surgery: a review of current methods," *Hepatobiliary & Pancreatic Diseases International*, vol. 17, no. 2, pp. 101–112, 2018.

[10] A. R. Gordon, J. E. Schreiber, A. Patel, and O. M. Tepper, "3D printed surgical guides applied in rhinoplasty to help obtain ideal nasal profile," *Aesthetic Plastic Surgery*, vol. 45, no. 6, pp. 2852–2859, 2021.

[11] W. S. Lin, J. C. Chou, J. R. Charette, M. J. Metz, B. T. Harris, and N. Choi, "Creating virtual 3-dimensional models for teaching pre-clinical tooth preparation: students' usages and perceptions," *European Journal of Dental Education*, vol. 22, no. 3, pp. e573–e581, 2018.

[12] I. D. Keenan and A. B. Awadh, "Integrating 3D visualisation technologies in undergraduate anatomy education," *Biomedical Visualisation*, vol. 1120, pp. 39–53, 2019.

[13] W. Fang, E. Gu, W. Yi, W. Wang, and V. S. Sheng, "A new method of image restoration technology based on WGAN," *Computer Systems Science and Engineering*, vol. 41, no. 2, pp. 689–698, 2022.

[14] S. Kadambi, Z. Wang, and E. Xing, "WGAN domain adaptation for the joint optic disc-and-cup segmentation in fundus images," *International Journal of Computer Assisted Radiology and Surgery*, vol. 15, no. 7, pp. 1205–1213, 2020.

[15] G. Lazaridis, M. Lorenzi, S. Ourselin, and D. Garway-Heath, "Improving statistical power of glaucoma clinical trials using an ensemble of cyclical generative adversarial networks," *Medical Image Analysis*, vol. 68, article 101906, 2021.

[16] M. Li, Q. Du, L. Duan et al., "Incorporation of residual attention modules into two neural networks for low-dose CT denoising," *Medical Physics*, vol. 48, no. 6, pp. 2973–2990, 2021.

[17] F. Deng, Q. Wan, Y. Zeng et al., "Image restoration of motion artifacts in cardiac arteries and vessels based on a generative adversarial network," *Quantitative Imaging in Medicine and Surgery*, vol. 12, no. 5, pp. 2755–2766, 2022.

[18] Y. Xiao, J. Wu, and Z. Lin, "Cancer diagnosis using generative adversarial networks based on deep learning from imbalanced data," *Computers in Biology and Medicine*, vol. 135, article 104540, 2021.

[19] S. Lee, J. Kim, G. Lee, J. Hong, J. H. Bae, and K. J. Lim, "Prediction of aquatic ecosystem health indices through machine learning models using the WGAN-based data augmentation method," *Sustainability*, vol. 13, no. 18, p. 10435, 2021.

[20] S. Gao, S. Qiu, Z. Ma, R. Tian, and Y. Liu, "SVAE-WGAN-based soft sensor data supplement method for process industry," *IEEE Sensors Journal*, vol. 22, no. 1, pp. 601–610, 2022.

[21] M. Zhang, Y. Zhang, Z. Jiang, X. Lv, and C. Guo, "Low-illumination image enhancement in the space environment based on the DC-WGAN algorithm," *Sensors*, vol. 21, no. 1, p. 286, 2021.

[22] J. Lee and H. Lee, "Improving SSH detection model using IPA time and WGAN-GP," *Computers & Security*, vol. 116, article 102672, 2022.

[23] M. Hu, M. He, W. Su, and A. Chehri, "A TextCNN and WGAN-gp based deep learning frame for unpaired text style transfer in multimedia services," *Multimedia Systems*, vol. 27, no. 4, pp. 723–732, 2021.

[24] K. Ning, Z. Zhang, K. Han, S. Han, and X. Zhang, "Multi-frame super-resolution algorithm based on a WGAN," *IEEE Access*, vol. 9, pp. 85839–85851, 2021.